Article

Luminescent Silole Nanoparticles as Chemoselective Sensors for Cr(VI)

Sarah J. Toal, Kelsey A. Jones, Douglas Magde, and William C. Trogler

J. Am. Chem. Soc., **2005**, 127 (33), 11661-11665• DOI: 10.1021/ja052582w • Publication Date (Web): 29 July 2005

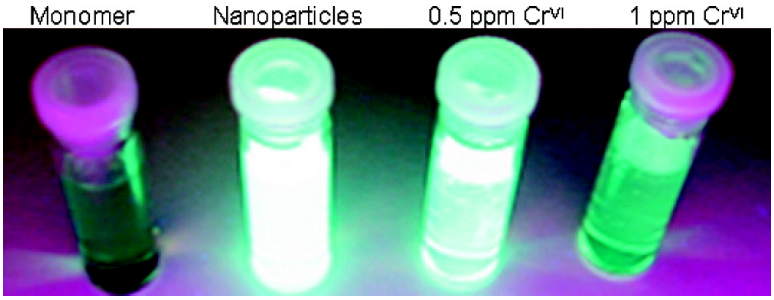

More About This Article

Additional resources and features associated with this article are available within the HTML version:

- Supporting Information
- Links to the 19 articles that cite this article, as of the time of this article download
- Access to high resolution figures
- Links to articles and content related to this article
- Copyright permission to reproduce figures and/or text from this article

View the Full Text HTML

J|A|C|S
ARTICLES
Published on Web 07/29/2005

Luminescent Silole Nanoparticles as Chemoselective Sensors for Cr(VI)

Sarah J. Toal, Kelsey A. Jones, Douglas Magde, and William C. Trogler*

Contribution from the University of California, San Diego, 9500 Gilman Drive, La Jolla, California 92093-0358

Received April 20, 2005; E-mail: wtrogler@ucsd.edu

Abstract: Colloidal suspensions of 3-aminopropylmethyl(tetraphenyl)silole nanoparticles can be used as selective chemosensors for carcinogenic chromium(VI) analyte. Methylhydrosilole is functionalized by hydrosilation of allylamine, and the colloid is prepared by the rapid addition of water to a THF solution of the silole. The method of detection is through electron-transfer quenching of the fluorescence of the silole colloid ($\lambda_{em} = 485$ nm at 360 nm excitation) by the analytes, with hundred parts per billion detection limits. Stern−Volmer plots are linear up to 10 ppm in the case of chromium, but exhibit saturation behavior near 5−10 ppm for arsenic. Dynamic light scattering experiments and AFM measurements show the particle sizes to be around 100 nm in diameter and dependent on solvent composition, with a particle size dispersity of ±25%. The fluorescence lifetimes of the silole in solution and colloid are ∼31 ps and ∼4.3 ns, respectively, while the silole has a lifetime of 6 ns in the bulk solid. A minimum volume fraction of 80% water is necessary to precipitate the colloid from THF, and the luminescence continues to rise with higher water fractions. Colloids in a pH 7 phosphate-buffered suspension show both higher sensitivity and greater selectivity (100-fold) for CrO_4^{2-} detection than for other oxoanion interferents, NO_3^-, NO_2^-, SO_4^{2-}, and ClO_4^-.

Introduction

Detection of chromium(VI) and arsenic(V) in drinking water is important because both species pose serious health risks and are regulated by the U.S. Environmental Protection Agency.[1] In aqueous solutions at pH 7, CrO_4^{2-}, which is isostructural with the sulfate ion, SO_4^{2-}, is carried into mammalian cells by sulfate transporters, where the CrO_4^{2-} oxidatively damages DNA.[2] Similarly, the predominant environmental form of As(V) in oxygenated water, AsO_4^{3-}, competes in cellular uptake with isoelectronic phosphate, PO_4^{3-}.[3] Both chromate and arsenate may be introduced into drinking water through industrial processes, as well as by environmental erosion.[1] The EPA has set the Maximum Contaminant Level Goals (MCLG) for total chromium and arsenic concentrations in drinking water at 100 and 10 ppb, respectively.[1] For chromium, it would be advantageous to be able to distinguish harmful Cr(VI) from benign Cr(III). There are currently several physical detection methods used to identify the presence of chromium and arsenic in aqueous media, including high performance liquid chromatography coupled with atomic absorption spectrometry,[4−6] fiber optic wave sensors,[7] ion chromatography,[8−10] inductively coupled plasma-MS,[11,12] electrochemical processes,[13,14] and electron capture GC.[15,16] Methods using luminescence quenching for detecting chromate have also been used. These include bacterial sensors[17] with detection limits as low as 2.6 ppb.[18] Dynamic quenching of luminescence in lanthanide complexes by chromate and nitrite using ion chromatography can detect 13 ppb of the anions.[19] A synchronous absorbance and fluorescence analysis of dynamic liquid drops at the end of a flow injection capillary, monitoring the decrease in fluorescence caused by the reaction between chromate and 3,3′,5,5′-tetramethylbenzidine dichloride, can detect chromate at the femtomolar level.[20]

Both chromate and arsenate are oxidants, a property that may be exploited to detect their presence in water. Recently, it was

(1) EPA list of drinking water contaminants and MCLs. http://www.epa.gov/safewater/mcl.html#mcls.
(2) Lippard, S. J.; Berg, J. M. *Principles of Bioinorganic Chemistry*; University Science Books: Mill Valley, CA, 1994.
(3) Kaim, W. S. B. *Bioinorganic Chemistry: Inorganic Elements in the Chemistry of Life*; John Wiley & Sons: New York, 1994.
(4) Syty, A.; Christensen, R. G.; Rains, T. C. *J. Anal. At. Spectrom.* **1988**, *3*, 193−197.
(5) Shuvaeva, O. V.; Koshcheeva, O. S.; Beisel, N. F. *J. Anal. Chem.* (Translation of Zhurnal Analiticheskoi Khimii) **2002**, *57*, 1037−1041.
(6) Niedzielski, P.; Siepak, M.; Novotny, K. *Central Eur. J. Chem.* **2004**, *2*, 82−90.
(7) Suresh Kumar, P.; Thomas Lee, S.; Vallabhan, C. P. G.; Nampoori, V. P. N.; Radhakrishnan, P. *Opt. Commun.* **2002**, *214*, 25−30.
(8) Gammelgaard, B.; Liao, Y.-p.; Jons, O. *Anal. Chim. Acta* **1997**, *354*, 107−113.
(9) Ganeshjeevan, R.; Chandrasekar, R.; Yuvaraj, S.; Radhakrishnan, G. *J. Chrom. A* **2003**, *988*, 151−159.
(10) Butler, E. C. V. *J. Chrom.* **1988**, *450*, 353−360.
(11) Yu, C.; Cai, Q.; Guo, Z.-X.; Yang, Z.; Khoo, S. B. *Spectrochim. Acta* **2003**, *58B*, 1335−1349.
(12) Magnuson, M. L.; Creed, J. T.; Brockhoff, C. A. *J. Anal. At. Spectrom.* **1997**, *12*, 689−695.
(13) Fuoco, R.; Papoff, P. *Ann. Chim.* **1975**, *65*, 155−63.
(14) Simm, A. O.; Banks, C. E.; Compton, R. G. *Anal. Chem.* **2004**, *76*, 5051−5055.
(15) Mugo, R. K.; Orians, K. J. *Anal. Chim. Acta* **1992**, *271*, 1−9.
(16) Cutter, L. S.; Cutter, G. A.; San Diego-McGlone, M. L. C. *Anal. Chem.* **1991**, *63*, 1138−1142.
(17) Peitzsch, N.; Eberz, G.; Nies, D. H. *Appl. Environ. Microbiol.* **1998**, *64*, 453−458.
(18) Ivask, A.; Virta, M.; Kahru, A. *Soil Biol. Biochem.* **2002**, *34*, 1439−1447.
(19) Schreurs, M.; Somsen, G. W.; Gooijer, C.; Velthorst, N. H.; Frei, R. W. *J. Chrom. A* **1989**, *482*, 351−359.
(20) Xiao, D.; Wang, K.; Xiao, W. *Analyst* **2001**, *126*, 1387−1392.

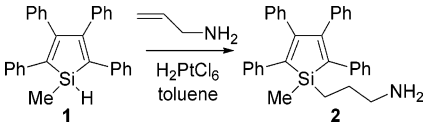

Figure 1. Synthesis of siloleamine chemosensor.

reported that silole-containing polymers are selective sensors for nitroaromatic oxidants, including TNT.[21,22] Detection is achieved though fluorescence quenching of the silole by the electron-deficient analyte. The silole luminescence is due to a $\sigma^*-\pi^*$ LUMO stabilized though conjugation of the σ^* orbital of the silicon chain with the π^* orbital of the butadiene moiety.[23] The selectivity of the sensor is due to the polymer's helical structure, which permits intercalation of planar nitroaromatics.[22] The aim of the research reported herein is to make a luminescent silole sensor for aqueous CrO_4^{2-} and AsO_4^{3-} by functionalization of a silole monomer with anion binding groups. Recently, it has been reported that colloidal suspensions of methylphenylsilole may be prepared by the rapid addition of water to an ethanolic silole solution, and that the colloid exhibits as much as a 300-fold increase in fluorescence intensity as compared to that in the organic solution.[24] Other silole colloids have since been prepared and characterized.[25] As most nanoparticles characterized in the literature are either purely inorganic,[26] such as semiconductor quantum dots,[27] or purely organic (e.g., carotenes[28] and dendrimers[29]), the silole organometallic nanoparticles are of particular interest for their unique photophysical and structural properties, as well as for their sensor applications. Fluorescent inorganic quantum dots have been shown to be widely useful in sensing applications.[30,31] This paper describes the potential utility of luminescent silole nanoparticles in redox sensing applications. An attractive feature of these molecular-based materials is their ease of functionalization for analyte recognition.

Results and Discussion

To make the silole nanoparticles bind oxoanions, such as CrO_4^{2-} and AsO_4^{3-}, a hydrogen-bonding amine functionality was incorporated into the monomer via a chloroplatinic acid (H_2PtCl_6)-catalyzed hydrosilation[32−34] of allylamine with methylhydrosilole, **1**, yielding the siloleamine, **2**, in 90% yield (Figure 1).

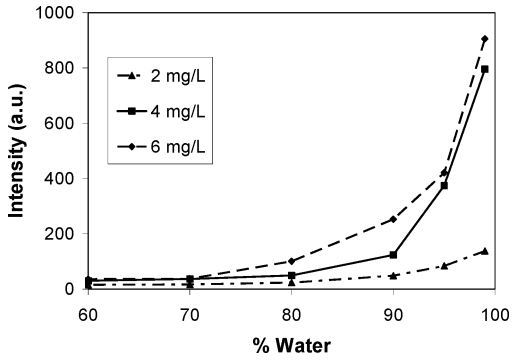

Figure 2. Fluorescence intensity for **2** in THF/H_2O as a function of water percentage.

The UV−vis absorption at 360 nm (ϵ = 7900 L/mol·cm), assigned to the $\pi-\pi^*$ transition of the silole moiety, is typical of tetraphenylsilole monomers.[35] A powder sample of **2** luminesces a bright yellow−green at 480 nm when excited at 360 nm; however, a THF solution of **2** is only weakly luminescent at 475 nm. The fluorescence quantum yield of **2** in toluene, measured relative to 9,10-diphenylanthracene,[36] is only $(1.15 \pm 0.35) \times 10^{-3}$, which is similar to the quantum yields of other silole monomers.[37] However, a dramatic increase in luminescence is observed for colloids of **2**, which are prepared by adding water rapidly to a THF solution of **2**. This rise in luminescence is accompanied by a 10 nm red shift in emission wavelength to 485 nm.

Luminescence of the colloid is highly dependent on solvent composition, specifically the amount of water used to precipitate **2**. Solutions containing 2, 4, and 6 mg/L of **2** in THF/H_2O were prepared at various water percentages. The concentration represents the total mass of silole, not the mass of the nanoparticles. A minimum volume fraction of 80% water is necessary to effect a detectable increase in luminescence (Figure 2). The luminescence continues to increase with 90, 95, and 99% water. For the 99% water samples, fluorescence rose by a factor of 15× for 2 mg/L, 36× for 4 mg/L, and 46× for 6 mg/L as compared with pure THF solutions of the respective concentration.

The colloids consist of particles on the order of 100 nm in size, as determined by dynamic light scattering measurements. Best fits to the data suggest a polydispersity of not more than ±25%. AFM images of settled particles show similar particle sizes. The colloid particles exhibit a minimum in size at 90% water, with somewhat larger sizes at both greater and lesser volume fractions of water. One possible explanation is that at higher water concentrations the organic silole molecules aggregate to a higher extent in the hydrophilic environment. The larger colloid particles observed at lower water concentrations may possibly be explained by THF absorbing into the particles causing them to swell.

Fluorescent lifetime measurements were performed to compare the dissolved silole and the silole in colloidal suspensions. In toluene solution, the fluorescence lifetime of **2** is only 31 ± 2 ps, which is somewhat longer than the lifetimes of both dimethyl(tetraphenyl)silole at 17.5 ± 2.5 ps, and hexaphenyl-

(21) Sohn, H.; Calhoun, R. M.; Sailor, M. J.; Trogler, W. C. *Angew. Chem., Int. Ed.* **2001**, *40*, 2104−2105.
(22) Sohn, H.; Sailor, M. J.; Magde, D.; Trogler, W. C. *J. Am. Chem. Soc.* **2003**, *125*, 3821−3830.
(23) Rappoport, Z.; Apeloig, Y. *The Chemistry of Organic Silicon Compounds*; John Wiley & Sons, LTD: New York, 2001; Vol. 3.
(24) Luo, J.; Xie, Z.; Lam, J. W.; Cheng, L.; Chen, H.; Qiu, C.; Kwok, H. S.; Zhan, X.; Liu, Y.; Zhu, D.; Tang, B. Z. *Chem. Commun.* **2001**, 1740−1741.
(25) Chen, J.; Law, C. C. W.; Lam, J. W. Y.; Dong, Y.; Lo, S. M. F.; Williams, I. D.; Zhu, D.; Tang, B. Z. *Chem. Mater.* **2003**, *15*, 1535−1546.
(26) Cushing, B. L.; Kolesnichenko, V. L.; O'Connor, C. J. *Chem. Rev.* **2004**, *104*, 3893−3946.
(27) Banin, U.; Millo, O. *Annu. Rev. Phys. Chem.* **2003**, *54*, 465−492.
(28) Horn, D.; Rieger, J. *Angew. Chem., Int. Ed.* **2001**, *40*, 4330−4361.
(29) Lemcoff, N. G.; Spurlin, T. A.; Gewirth, A. A.; Zimmerman, S. C.; Beil, J. B.; Elmer, S. L.; Vandeveer, H. G. *J. Am. Chem. Soc.* **2004**, *126*, 11420−11421.
(30) Lian, W.; Litherland, S. A.; Badrane, H.; Tan, W.; Wu, D.; Baker, H. V.; Gulig, P. A.; Lim, D. V.; Jin, S. *Anal. Biochem.* **2004**, *334*, 135−144.
(31) Lin, C. I.; Joseph, A. K.; Chang, C. K.; Lee, Y. D. *J. Chrom. A* **2004**, *1027*, 259−262.
(32) Benkeser, R. A.; Cunico, R. F.; Dunny, S.; Jones, P. R.; Nerlekar, P. G. *J. Org. Chem.* **1967**, *32*, 2634−2636.
(33) Kim, D. S.; Shim, S. C. *J. Polym. Sci., Part A: Polym. Chem.* **1999**, *37*, 2933−2940.
(34) Onopchenko, A.; Sabourin, E. T. *J. Org. Chem.* **1987**, *52*, 4118−4121.
(35) Dubac, J.; Laporterie, A.; Manuel, G. *Chem. Rev.* **1990**, *90*, 215−263.
(36) Morris, J. V.; Mahaney, M. A.; Huber, J. R. *J. Phys. Chem.* **1976**, *80*, 969−974.
(37) Toal, S. J.; Sohn, H.; Zakarov, L. N.; Kassel, W. S.; Golen, J. A.; Rheingold, A. L.; Trogler, W. C. *Organometallics* **2005**, *24*, 3081−3087.

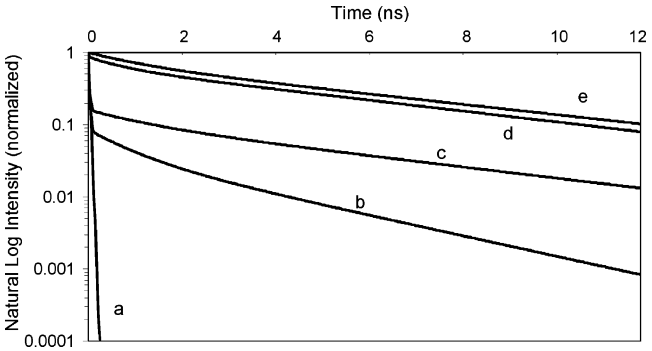

Figure 3. Semilog plots of fluorescence lifetime decay of **2**, 6 mg/L, in THF/water solutions for (a) 0%, (b) 80%, (c) 90%, (d) 95%, and (e) 99% water. Amplitudes are normalized, so all curves begin at 1.

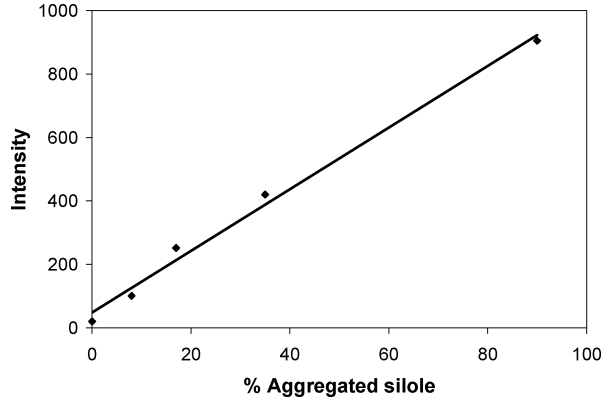

Figure 4. Fluorescence intensity as a function of percent aggregated **2** for a 6 mg/L colloid. The percentage of aggregated silole was determined from the fluorescence decay curves.

silole, whose reported lifetime in acetone is 20 ps.[38] Intramolecular quenching of the $\pi-\pi^*$ excited state of the silole by the donor amino moiety is, therefore, not responsible for the short lifetime in the siloleamine. Indeed, the luminescence of polysiloles is quenched by electron acceptors, rather than by electron donors.[22] The lifetime of **2** is about 20 times shorter than that observed for poly(tetraphenyl)silole at 700 ps.[22] The polysilole adopts a helical structure, and solvent access to the face of the silole π system is restricted. This may account for the long fluorescence lifetime observed for the polymer and for siloles in the solid state. Other workers have attributed the increased lifetime of silole monomers in the solid state to restricted rotation of the phenyl substituents.[24,38] As water is added and the nanoparticles begin to form, fluorescence emission lifetimes become longer and are clearly nonexponential. Multiexponential fits of fluorescence decay curves show a fast decay component from unaggregated species still present in the colloidal suspension, along with additional longer decay time components from the nanoparticle aggregates. Figure 3 shows semilog plots of the fluorescence decay curves of 6 mg/L solutions at various water concentrations. The nanoparticles have mean lifetimes of 4.0, 4.3, and 4.6 ns in 90, 95, and 99% water solutions, respectively. The lifetime reported is an average of two exponentials needed to obtain an appropriate fit to the nanoaggregate decay. This is not surprising, as the particles are not uniform in size, but span a size distribution. The longest-lived nanoparticles observed have a fluorescence lifetime of 6 ns, which is also the lifetime of **2** in the solid state.

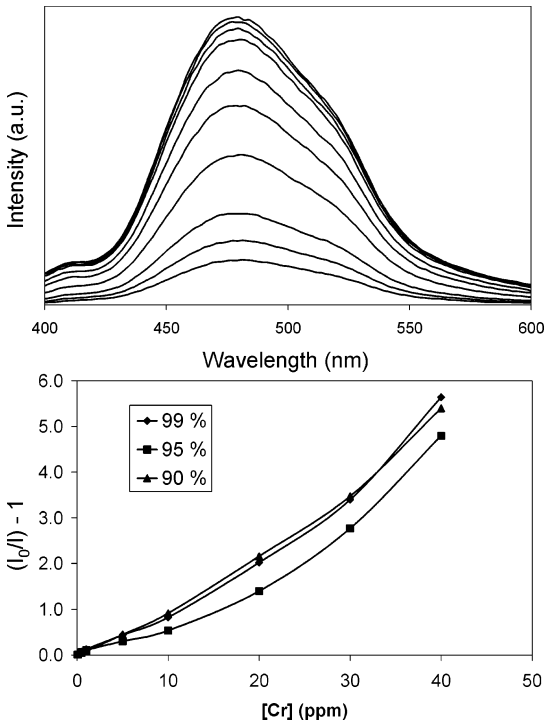

Figure 5. Photoluminescence quenching of 4 mg/L of **2** by CrO_4^{2-}: (top) quenching by, from top, 0, 0.1, 0.5, 1, 2.5, 5, 10, 20, 30, and 40 ppm quencher in 90% water; (bottom) Stern−Volmer plots of photoluminescence quenching in various water percentages.

The unaggregated **2** is readily distinguished in Figure 3 because of its very short lifetime, as compared to the nanoparticles. In an 80% water suspension, 92% of the silole remains dissolved, as can be seen in Figure 3b with the sharp initial decay. In 90% water, 83% silole remains dissolved, and in 95% water, 65% of the silole remains dissolved. In a 99% water suspension, less than 10% of **2** is in solution.[39] The luminescence intensity is also directly proportional to the percent of aggregated silole (Figure 4), as determined from the lifetime analysis. The nonzero intercept in Figure 4 corresponds to the weak fluorescence contribution arising from the solution phase silole.

The ability of the siloleamine to detect the carcinogens CrO_4^{2-} and AsO_4^{3-} was investigated by adding successive aliquots of aqueous stock solutions of the analytes to nanoparticle suspensions of **2** and monitoring the decrease in fluorescence intensity (Figures 5 and 6 (top), respectively). Quenching of photoluminescence is observed at the EPA action level of 0.1 ppm CrO_4^{2-}. Not surprisingly, since AsO_4^{3-} is a weaker oxidant than CrO_4^{2-}, it is a weaker quencher as well (standard reduction potentials vs NHE are -0.68 and -0.13 V, respectively, and at pH 7 they are $+0.15$ and $+0.56$ V, respectively).[40] This supports the hypothesis that the quenching of photoluminescence of siloles is due to electron transfer from the excited state of the silole to the analyte.

(38) Lee, M. H.; Kim, D.; Dong, Y.; Tang, B. Z. *J. Korean Phys. Soc.* **2004**, *45*, 329−332.

(39) This assumes that the quantum yields of the aggregates and unaggregated silole are proportional to τ_{obs}/τ_{rad}, where τ_{obs} is the observed lifetime and τ_{rad} is the radiative lifetime. The radiative lifetimes are assumed to be the same for both species because their absorption and emission spectra are nearly identical.

(40) Huheey, J. E.; Keiter, E. A.; Keiter, R. L. *Inorganic Chemistry: Principles of Structure and Reactivity*, 4th ed; HarperCollins College Publishers: New York, 1993.

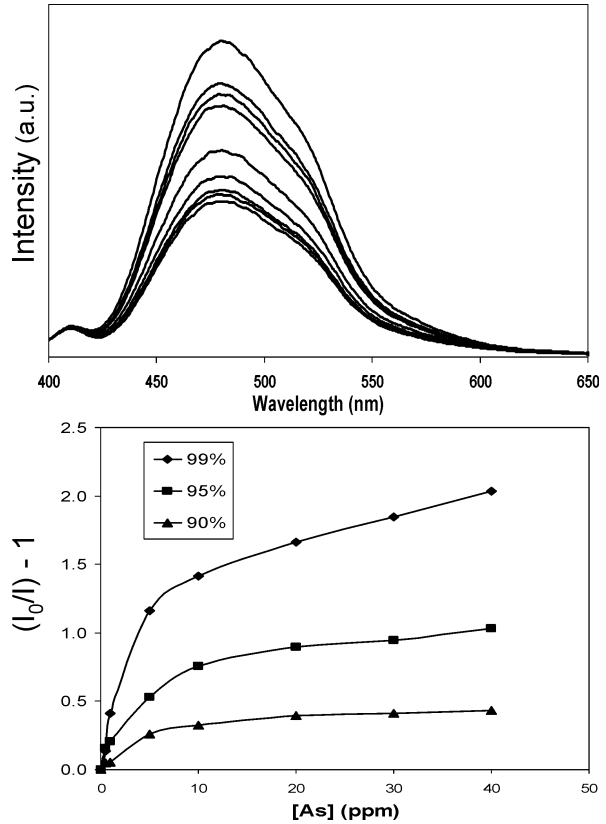

Figure 6. Photoluminescence quenching of 4 mg/L of **2** by AsO_4^{3-}: (top) quenching by, from top, 0, 0.5, 1, 2.25, 5, 10, 20, 30, and 40 ppm quencher in 95% water; (bottom) Stern−Volmer plots of photoluminescence quenching in various water percentages.

Quenching efficiencies were fit to the Stern−Volmer equation, $I_0/I = K_{SV}[A] + 1$, which relates the fluorescence intensity, I, at different concentrations of analyte quencher, [A], where I_0 is the intensity at [A] = 0, and K_{SV} is the Stern−Volmer constant. A plot of CrO_4^{2-} quenching efficiency is linear up to 10 ppm, at which point there is a rise in quenching efficiency (Figure 5, bottom). However, a Stern−Volmer plot of AsO_4^{3-} quenching saturates above 10 ppm (Figure 6, bottom). The nonlinear relationship observed for arsenate may indicate saturation of the surface-binding sites since the nanoparticle concentration per liter is approximately 6×10^{12}, which is less than the analyte molecular concentration per liter of approximately 4×10^{18} at 1 ppm AsO_4^{3-}. It also suggests that the lower driving force for electron transfer with AsO_4^{3-} does not permit complete quenching at saturation coverage of the nanoparticles.

The selectivity of the colloid sensor was tested by performing quenching experiments in pH 7 phosphate-buffered suspensions, using both CrO_4^{2-} and AsO_4^{3-}, as well as common aqueous interferents, NO_3^-, NO_2^-, SO_4^{2-}, and ClO_4^-. Colloids prepared in the buffer were almost twice as luminescent as those prepared in distilled water since the presence of phosphate alone led to an increase in nanoparticle luminescence. The buffer was used in the interferent quenching studies in order to prevent variations in the fluorescence intensity caused by changes in ionic strength from quenchers at higher concentrations (>50 ppm). Sensitivity to Cr(VI) detection more than doubled in the buffered aqueous colloid as compared to that of the unbuffered suspensions. Even though phosphate anions may compete with chromate for surface hydrogen bonding sites, the increased luminescence intensity more than compensates for any sensitivity loss. Stern−Volmer plots of Cr(VI) quenching in the buffered aqueous colloid are linear only up to 1 ppm, after which there is a sharp rise in sensitivity. This may be due to competition between the chromate quencher and phosphate buffer for binding sites at lower chromate concentrations. However, sensitivity to arsenate decreased about 20-fold for the buffered colloid, which suggests that phosphate effectively competes with arsenate. Much higher concentrations of the interferent analytes (NO_3^-, NO_2^-, SO_4^{2-}, and ClO_4^-) were needed to observe quenching. Comparison of the slopes of Stern−Volmer plots gives relative sensitivities to analyte detection. For instance, the buffered colloid is 120 times more sensitive to chromate than to nitrate. A summary of the relative sensitivities is shown in Table 1. The net result is that preparation of the colloid of **2** with a pH 7 phosphate buffer produces a highly selective chromate sensor.

Table 1. Stern−Volmer Constants and Relative Sensitivities of a pH 7 Phosphate-Buffered Colloid of **2** to Various Aqueous Anions

analyte	Stern−Volmer constant (M^{-1})	relative sensitivity
NO_3^-	87	1.0
ClO_4^-	140	1.6
SO_4^{2-}	170	2.0
NO_2^-	780	9.0
AsO_4^{3-}	1300	15
CrO_4^{2-}	10900	120

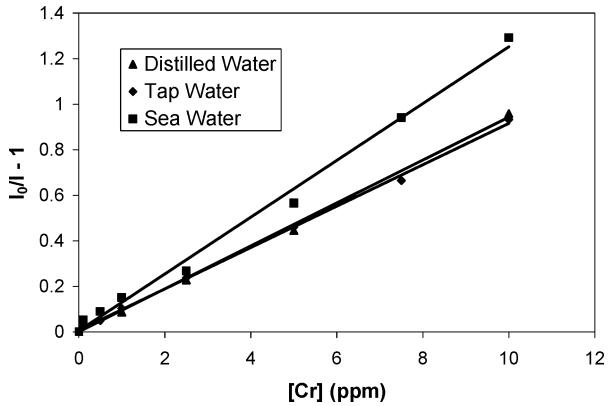

Figure 7. Stern−Volmer plots of luminescence quenching of **2**, 4 mg/L, in 90% water suspension, by chromate.

Quenching experiments were also carried out on environmental water samples to determine the ability of the silole to detect chromate in the presence of ambient interferents at actual environmental concentrations. Quenching efficiencies for chromate spiked in San Diego tap water were identical to those measured in distilled water, and efficiencies for chromate spiked in La Jolla seawater were only slightly higher (Figure 7). The higher sensitivity to chromate in the saline seawater, with its high ionic strength, is in agreement with the observation that buffered suspensions also provide more sensitive chromate detection.

Experimental Section

General. All synthetic manipulations were carried out under an atmosphere of dry argon gas using standard Schlenk techniques. Solvents were purchased from Aldrich Chemical Co. Inc. and distilled from sodium/benzophenone ketyl. NMR data were collected with Varian Unity 300 or 500 MHz spectrometers (300.1 MHz for ^1H, 77.5 MHz

for ^{13}C, and 99.4 MHz for ^{29}Si NMR). Fluorescence emission and excitation spectra were recorded with the use of a Perkin-Elmer LS 50B luminescence spectrometer. UV−vis spectra were obtained with the use of a Hewlett-Packard 8452A diode array spectrometer. Atomic force microscopy images of particles settled on glass slides were obtained with the use of a Digital Instruments Nanoscope IIIa. Fluorescence lifetimes were measured using time-correlated photon counting, following excitation by the frequency-doubled output of a mode-locked Ti:sapphire laser, as described previously.[22] Dynamic light scattering[41] used an argon ion laser line at 514.5 nm, with detection at 90° in a solid angle of one or two coherence areas. Individual photons were detected and recorded in bin-widths of 10 μs and correlation functions calculated by digital computer, assuming spherical particles. Although the particle diffusion can be obtained through first principles, the calibration was verified by measuring latex spheres of known diameters.

1-Methyl-1-(3-amino)propyl-2,3,4,5-tetraphenylsilole (2): Methylhydrosilole[42] (1.0 g, 2.5 mmol), allylamine (0.36 mL, 5.0 mmol), $H_2PtCl_6 \cdot xH_2O$ (2.5 mg, 5 μmol), and freshly distilled toluene (10 mL) were placed under an Ar atmosphere and refluxed for 20 h. The solution was cooled, passed through a sintered glass frit, and evaporated to dryness. The product was dissolved in ether and precipitated with hexanes and filtered. The precipitate, **2**, was collected as a yellow powder: (1.1 g, 90%); ^1H NMR (300 MHz, $CDCl_3$ ($\delta = 7.26$)) $\delta =$ 6.7−7.3 (m, 20H, Ph), 2.64 (t, 2H), 1.53 (m, 2H), 1.01 (m, 2H), 0.49 (s, 3H); ^{13}C NMR (100 MHz, $CDCl_3$ ($\delta = 77.00$)) $\delta =$ 154.638, 140.784, 139.691, 138.523, 129.802, 128.685, 127.838, 127.254, 126.079, 125.419, 44.847, 27.367, 10.593, 4.587; ^{29}Si NMR (99.36 MHz, INEPT, $CDCl_3$, TMS ($\delta = 0.0$)) $\delta = 9.5$; MS(ES) m/z 458.8 [M + 1]; CHN (w/O_2 purge) $C_{32}H_{31}SiN \cdot H_2O$, calcd C 80.79, H 6.99, N 2.94; found C 81.40, H 6.99, N 2.80.

Acknowledgment. We thank the Environmental Protection Agency (Grant R829619) and the National Science Foundation (Grant CHE-0111376) for financial support. S.J.T. also thanks the San Diego chapter of Achievement Rewards for Collegiate Scientists for a fellowship. D.M. thanks the late Professor K. Wilson.

JA052582W

(41) Berne, B. J.; Pecora, R. *Dynamic Light Scattering*; John Wiley and Sons: New York, 1976.
(42) Ruhlmann, K. *Z. Chem.* **1965**, *5*, 354.